Journal of Physics D: Applied Physics

Modeling the physics of interaction of high-pressure arcs with their electrodes: advances and challenges

To cite this article before publication: Mikhail S Benilov 2019 *J. Phys. D: Appl. Phys.* in press https://doi.org/10.1088/1361-6463/ab47be

Modeling the physics of interaction of high-pressure arcs with their electrodes: advances and challenges

M. S. Benilov
Departamento de Física, Faculdade de Ciências Exatas e da Engenharia, Universidade da Madeira, Largo do Município, 9000 Funchal, Portugal
Instituto de Plasmas e Fusão Nuclear, Instituto Superior Técnico, Universidade de Lisboa, 1041 Lisboa, Portugal
email *benilov@staff.uma.pt*

Abstract

Incorporation of realistic models of plasma-electrode interaction remains a bottleneck in the development of predictive models of devices with high-pressure arcs. The most important aspects of the underlying physics have already been understood, so no fundamentally new physical mechanisms have been described in the recent publications (which are many); the aim was rather to develop practicable numerical models that adequately describe known mechanisms. Unfortunately, no universally accepted numerical models have emerged: the developed models are in many cases incompatible with each other and it is not easy to identify the place of each model in the global picture. The aim of this contribution is to summarize physically justified descriptions of the interaction of high-pressure arcs with their electrodes and to survey from this point of view the recent works, thus bringing them into a kind of system insofar as possible. The relevant aspects of the conventional LTE arc models are discussed. Outstanding challenges for future work are identified.

Keywords: high-pressure arcs, near-electrode phenomena, arc-electrode interaction

1 Introduction

Incorporation of realistic models of plasma-electrode interaction remains a bottleneck in the development of predictive models of devices with high-pressure arcs; e.g., reviews [1–4]. This explains the recent surge of interest in the modelling of plasma-electrode interaction in high-pressure arc discharges: limiting oneself to works published since 2016 and setting aside papers in this Special Issue, one can mention journal papers [5–35], a review paper [36], and PhD theses [37–40]. The most important aspects of physics of current transfer to electrodes of arc discharges have been understood quite some time ago, so no fundamentally new physical mechanisms have been described in recent publications; the goal was rather to develop practically feasible numerical models that adequately describe known mechanisms.

Unfortunately, no universally accepted numerical models have emerged: the developed models are in many cases incompatible with each other and it is not easy to identify the place of each model in the global picture. This is in stark contrast with the modelling of the arc bulk,

where well-established magnetohydrodynamics (MHD) models are used. The reason is two-fold. Firstly, the physics of arc-electrode interaction is objectively more complex and diverse than the arc bulk physics. Secondly, it is an applied field and some authors are not interested in the physical validity and self-consistency of their models; they evoke more or less arbitrary relationships and consider the agreement with some or other experiment to be the ultimate justification.

The aim of this contribution is to summarize physically justified descriptions of the interaction of high-pressure arcs with their electrodes and to survey from this point of view the recent works, thus bringing them into a kind of system insofar as possible. Of course, models that are not physically justified do not fit this classification. However, this classification provides a 'coordinate system' and in this sense can be useful for understanding also such models.

The outline of the paper is as follows. Different ways of self-consistent description of high-pressure arc plasmas in their interaction with solid surfaces are considered in section 2. In particular, conditions are formulated for a model used for non-equilibrium layers, separating the arc bulk from solid surfaces, to be consistent with the model used for the arc bulk. A classification of different self-consistent numerical models of arcs on the whole, resulting from this consideration, is discussed. In section 3, a survey of existing numerical models of high-pressure arc discharges and their interaction with electrodes is given, with emphasis on most recent works. In section 4, results given by different self-consistent approaches are compared with each other and the relevant aspects of the conventional LTE models are discussed. Conclusions are summarized in section 5.

2 Describing the physics of interaction of high-pressure arc plasmas with solid surfaces

2.1 Unified description

There is a well developed and universally used fluid description of cold discharges, e.g., glow, radiofrequency, dielectric barrier, corona, and streamer discharges. The system of differential equations includes equations of conservation of species; equations of transport of species, which are written in the form of Fick's law with account of drift of the charged particles in the electric field (the so-called drift-diffusion approximation), unless the plasma pressure is very low; the Poisson equation, relating the electric field to the plasma space charge; equation of energy for the electron species; and the continuity, momentum (Navier-Stokes), and energy equations for the plasma on the whole. Other equations may be included as needed, e.g., equations of radiation transport for evaluation of photoionization and equation of conservation of surface electric charge on dielectric surfaces. This system of equations is solved in the whole plasma computation domain up to solid surfaces, including the electrodes, and there is no need to subdivide the plasma into the bulk and near-electrode regions.

The same system of equations, with appropriate modifications, describes plasmas of arc discharges in high-pressure gases. Since the ionization degree of plasmas of high-current arc discharges is comparable to unity, transport of the arc plasma species is affected by the multicomponent diffusion. Therefore, Fick's law (drift-diffusion) equations have to be replaced by equations taking into account the multicomponent diffusion. Since currents are high in arc discharges, the Lorentz force due to the self-induced magnetic field may play a role; e.g., the cathode jet phenomenon, also known as the Maecker effect. Therefore, Maxwell equations

describing the self-induced magnetic field have to be included into the system of governing differential equations. Since energy fluxes from arc plasmas to electrodes are quite high, equations of heat conduction inside the electrodes have to be included. Another consequence of high currents may be a significant Joule effect inside the electrodes, hence the equation of current continuity inside electrodes, supplemented with Ohm's law, has to be included.

One can think of developing, on the basis of these equations, a straightforward approach to modelling of arc discharges: the single set of equations, including the Poisson equation, is employed in the whole interelectrode gap up to electrode surfaces. A defining feature of this straightforward, or unified, modelling approach is that it does not require the plasma computation domain to be divided into regions governed by different physical mechanisms, such as the quasi-neutral plasma and space-charge sheath. Therefore, there is no need to a priori theorize about governing mechanisms, which is a very important advantage of such approach. At the same time, this feature represents a limitation: arc discharges do contain regions governed by different physical mechanisms, which, strictly speaking, should not be described by a single system of equations. For example, collisionless near-cathode space-charge sheaths with two groups of electrons (those emitted by the cathode surface and electrons coming from the bulk plasma), strictly speaking, cannot be described by the same equations that the collision-dominated quasi-neutral plasma.

On the other hand, the unified modelling approach is highly computationally intense and its application has been very limited up to now.

2.2 Separate descriptions of the arc bulk and non-equilibrium layers near solid surfaces

An alternative to unified modelling is to employ separate descriptions of the arc bulk plasma and thin non-equilibrium layers near solid surfaces (electrodes and insulators). Some kind of equilibrium is assumed to hold in the bulk: the quasi-neutrality and/or ionization (Saha) equilibrium and/or thermal equilibrium (equilibrium between the electron and heavy-particle temperatures T_e and T_h). Deviations from the equilibrium are assumed to be confined to the near-surface non-equilibrium layers.

2.2.1 Characteristic length scales

Let us consider length scales characterizing deviations from the equilibria, considering an atomic plasma with singly charged ions as a representative example. Deviations from the quasi-neutrality are characterized by the Debye length λ_D. The ionization equilibrium is perturbed by ambipolar diffusion and/or by convective transport of the charged particles. Since we are interested primarily in perturbations occurring near solid surfaces and the convective velocity vanishes at solid surfaces, we assume that the convective transport is no stronger than the ambipolar diffusion and therefore does not need to be estimated separately. The dominant mechanism of ionization of neutral particles in atomic plasmas is electron impact ionization. Then the length scale on which the rate of transport of charged particles due to ambipolar diffusion is comparable to the ionization rate may be written as [41]

$$d = \frac{1}{C_2}\sqrt{\frac{D_a k T_h}{k_i p}}. \qquad (1)$$

Here D_a is the coefficient of ambipolar diffusion; C_2 is the dimensionless coefficient defined by equation (14) of [41], which depends on the ratio T_e/T_h and varies between approximately 0.67 and 1; and k_i is the ionization rate constant (the function of T_e). d is usually called the ionization length.

In arc plasmas, the energy transport by the electron heat conduction and electron current dominates over the energy transport by the heavy particles, except at very low arc currents where the ionization degree is of the order of 1% or lower. The translational energy exchange term is unessential in the electron energy equation and one can say that the electron temperature T_e is decoupled from the heavy-particle temperature T_h. The question of whether the thermal equilibrium holds amounts to whether the heavy-particle temperature follows the electron temperature (and not *vice versa*). In other words, a process perturbing thermal equilibrium is transport of the heavy-particle energy by the heat conduction and convection. (Note that the diffusion fluxes of the ions and the atoms compensate each other, hence the transport of the heavy-particle energy by the diffusion fluxes may be neglected.) As above, we are interested in deviations from (thermal) equilibrium near solid surfaces, and they occur on the length scale on which heavy-particle heat conduction is comparable to the rate of translational energy exchange between the electrons and the heavy particles. This scale may be written as [42]

$$L_{tn} = \sqrt{\frac{\kappa_h m_i}{k n_e m_e \bar{\nu}_{eh}}}. \tag{2}$$

Here and further n_e, n_i, and n_a are the number densities of the electrons, ions, and atoms; m_e and m_i are masses of the electrons and the atoms; and $\bar{\nu}_{eh}$ is the average frequency of momentum transfer in elastic collisions of an electron with heavy particles.

Another relevant length scale is the mean free path for collisions between the ions and neutral atoms:

$$\lambda_{ia} = \frac{1}{(n_a + n_i)\,\bar{Q}_{ia}^{(1,1)}}, \tag{3}$$

where $\bar{Q}_{ia}^{(1,1)}$ is the energy-averaged cross section for momentum transfer in ion-atom collisions. Note that λ_{ia} defined in this way represents the mean free path of an ion in the gas of atoms in the case of weakly ionized plasma, $n_i \ll n_a$, and the mean free path of an atom in the gas of ions in the case of plasma close to full ionization, $n_a \ll n_i$.

As an example, these length scales are shown, as functions of T_h and T_e, in figure 1 for the plasma of the atmospheric-pressure argon arc, which is a kind of standard example of a high-pressure arc discharge. In figure 2, the length scales are shown for mercury arc plasma under the pressure of 30 bar, which is relevant for high-intensity discharge (HID) lamps. The electron temperature T_e near solid surfaces may be as high as several eV. Figures 1(a) and 2(a) refer to conditions representative of the immediate vicinity of the surface, where the heavy-particle temperature T_h is close to the surface temperature. The conditions of figures 1(b) and 2(b) are representative for larger distances from the surface, where T_h is close to T_e.

While computing the data shown in figures 1 and 2, the charged particle densities have been evaluated by means of the Saha equation for given values of p, T_h, and T_e neglecting the presence of multiply charged ions. It is obvious that the latter is justified in the range of T_e up to 20,000 K, where the equilibrium densities of the multiply charged ions are small (below 0.7% and 1.2% of the density of the singly charged ions for 1 bar Ar at $T_h = 3,000$ K and $T_h = T_e$, respectively; similar numbers for 30 bar Hg are 1.4% and 2.4%). Of course, the equilibrium densities of the multiply charged ions are not small for higher values of T_e.

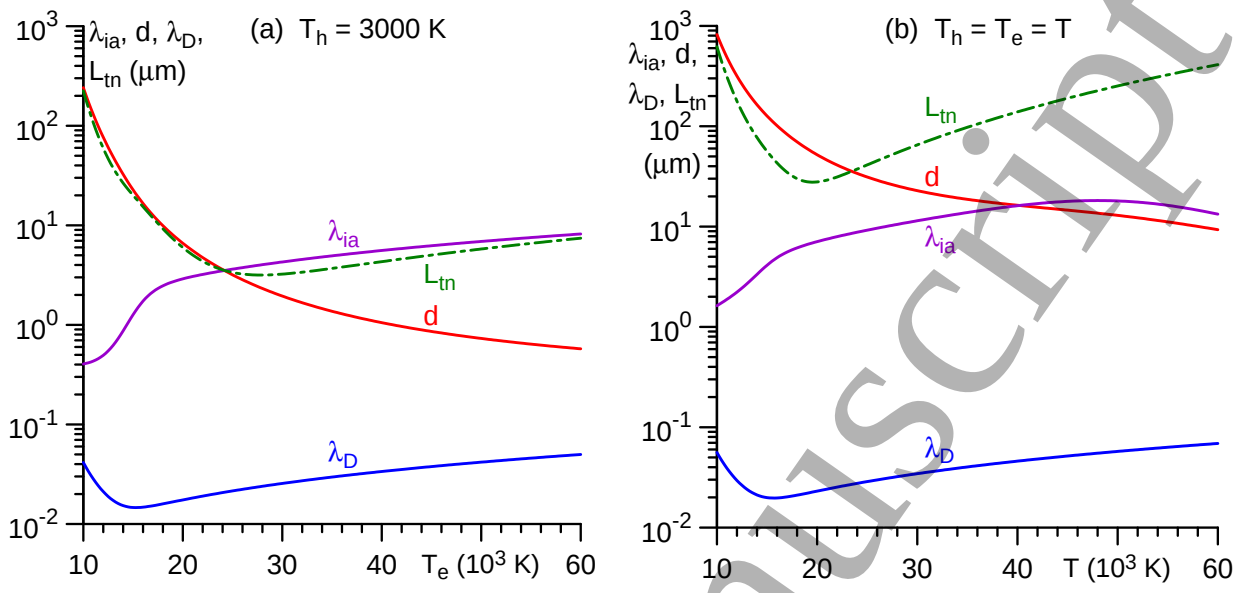

Figure 1. Characteristic length scales. Ar plasma, $p = 1$ bar.

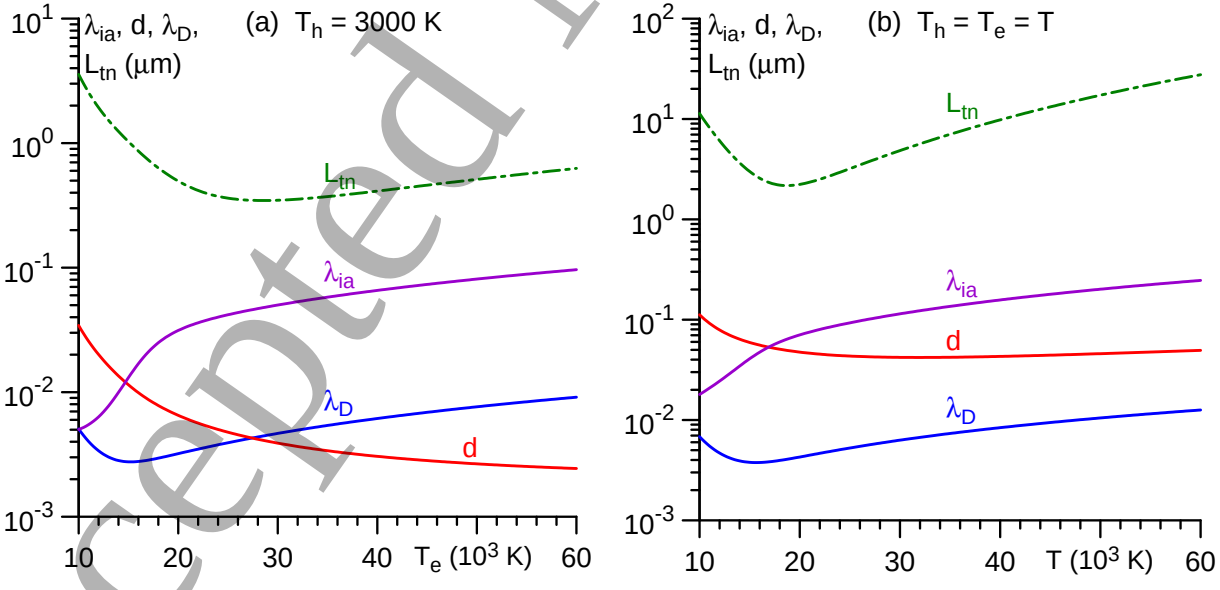

Figure 2. Characteristic length scales. Hg plasma, $p = 30$ bar.

However, numerical calculations of non-equilibrium distributions of atoms, electrons, singly, doubly, and triply charged ions in the near-cathode layer in the atmospheric-pressure argon plasma, reported in [43] for T_e in the range from 10,000 to 50,000 K, have shown that the dominating ion species in the near-surface region is Ar^+ in the whole electron temperature range considered. This is a consequence of the fact that the rate constant of each subsequent ionization decreases, which is a general tendency rather than a specific property of argon. One can expect therefore that this conclusion is not restricted only to atmospheric-pressure argon arcs but is instead a rather general one. This justifies the neglect of the multiply charged ions under conditions of figures 1 and 2.

The above length scales are useful for the purposes of qualitative analysis of sections 2.2.2 and 2.2.3 below. Moreover, these length scales can be useful for understanding the results of numerical simulations, as will be illustrated in section 3.1. Of course, there are limitations; for example, values of λ_D estimated at the edge of the non-equilibrium layer significantly underestimate the thickness of the near-cathode space-charge sheath, which will be illustrated in section 3.1 as well.

2.2.2 The arc bulk

The bulk plasma of high-pressure arc discharges has been described in the literature by a variety of models of different levels of complexity. Most works employ models based on the assumption of local thermodynamic equilibrium (LTE), which amounts to assuming quasi-neutrality, the ionization (Saha) equilibrium, and thermal equilibrium (equilibrium between the electron and heavy-particle temperatures T_e and T_h); e.g., reviews [1, 2, 4, 44]. The assumption of LTE is justified if

$$\lambda_D, d, L_{tn} \ll L, \tag{4}$$

where L is a characteristic dimension of the arc, e.g., a characteristic radius of the arc channel or the interelectrode distance, whichever is smaller.

Many papers employ the so-called two-temperature, or 2T, arc bulk description, which assumes quasi-neutrality and ionization equilibrium but takes into account thermal non-equilibrium, e.g., review [45]; works [46–48] may be mentioned as more recent examples. The criterion of applicability of the 2T models is $\lambda_D, d \ll L$, meaning that such models, in addition to being valid under the conditions of validity of the LTE approximation, defined by inequality (4), are also applicable in the case

$$\lambda_D, d \ll L_{tn}, L. \tag{5}$$

Since the LTE approximation is inapplicable in the case (5), the 2T description is the method of choice in this case.

Note that Ohm's law is written in the form $\mathbf{j} = \sigma\mathbf{E}$ in works dedicated to the modelling of LTE and 2T plasmas, except for those that take into account thermal diffusion. The account of the diffusion due to variations of the plasma composition was introduced in [49], in the same way as the effect of the diffusion over the energy transport in chemical-equilibrium mixtures is routinely taken into account by means of the reactive thermal conductivity. The result was a modification of Ohm's law in LTE and 2T plasmas: new terms proportional to the temperature gradient (or, in the case of 2T plasmas, to ∇T_e and ∇T_h) and to the plasma pressure gradient have appeared. One can hope that this modification will contribute to increasing the accuracy of the LTE and 2T descriptions of arc discharges, in particular, of the arc-anode interaction.

There are also papers which assume the quasi-neutrality and thermal equilibrium but take into account ionization non-equilibrium; e.g., [50–55]. The criterion of applicability of such

models is $\lambda_D, L_{tn} \ll L$, meaning that these models, in addition to remaining valid under the conditions of validity of the LTE approximation, are the method of choice in the case

$$\lambda_D, L_{tn} \ll d, L. \tag{6}$$

However, it is seen from figures 1 and 2 that the ionization length under typical conditions of arc plasmas is comparable to or smaller than the temperature relaxation length: $d \lesssim L_{tn}$. Hence, the usefulness of such models is limited.

Finally, there are models that assume only the quasi-neutrality and do not rely on assumptions of thermal or ionization equilibrium; e.g., [56–63]. The criterion of validity of these models is $\lambda_D \ll L$ and they are the method of choice in the case

$$\lambda_D \ll d, L_{tn}, L. \tag{7}$$

2.2.3 Near-surface non-equilibrium layers and their mathematical description

In each case, the model of near-surface non-equilibrium layers has to be consistent with the model used for description of the arc bulk plasma. Let us consider first the case where the arc bulk plasma is described by means of a model that relies only on the assumption of quasi-neutrality and accounts for the ionization and thermal non-equilibria. Then the only additional kind of non-equilibrium to be taken into account near a solid surface is the deviation from quasi-neutrality, i.e., charge separation, which occurs on distances of order of λ_D from the surface. In other words, the near-surface non-equilibrium layer represents a space-charge sheath in this case.

If the arc bulk plasma is described by means of a 2T model, which takes into account thermal non-equilibrium in the arc bulk but assumes ionization equilibrium and quasi-neutrality, two additional kinds of non-equilibrium are to be taken into account near a solid surface: a deviation from ionization equilibrium and charge separation. The thickness of the near-surface non-equilibrium layer in this case is of the order of the largest of the scales d and λ_D.

Finally, if the arc bulk plasma is described by means of an LTE model, then all the three kinds of non-equilibrium are to be taken into account near a solid surface: a deviation from thermal equilibrium, a deviation from ionization equilibrium, and charge separation. The thickness of the near-surface non-equilibrium layer in this case is of the order of the largest of the scales L_{tn}, d, and λ_D.

Thus, in each approach with separate descriptions of the arc bulk and near-surface non-equilibrium layers, the physics accounted for in the non-equilibrium layer has to be consistent with the description of the arc bulk. Moreover, the way in which the non-equilibrium layers are introduced in the mathematical model of the arc on the whole has to be consistent with the arc bulk description as well. Again, let us start with the case where the arc bulk plasma description relies only on the assumption of quasi-neutrality. As discussed above, the near-surface non-equilibrium layer represents a space-charge sheath in the framework of this approach and has the thickness of the order of λ_D. Firstly, since terms that are small in the parameter λ_D/L are neglected, i.e., considered to be infinitely small in the quasi-neutral arc bulk description, such terms must be considered as infinitely small also in the description of the near-surface space-charge sheath, in order for the model of the arc on the whole to be consistent. It follows that the sheath should be introduced in the mathematical model of the arc on the whole as an infinitesimally thin interface separating the quasi-neutral arc bulk plasma from the solid surface.

Secondly, the quasi-neutral arc bulk description, being inapplicable on length scales of the order of λ_D or smaller, correctly describes deviations from ionization and thermal equilibrium only if the length scales d and L_{tn}, on which these deviations occur, are much larger than λ_D. In other words, terms that are small in the parameters λ_D/d and λ_D/L_{tn} are not taken into account in the quasi-neutral arc bulk description. Hence, such terms must be neglected in the description of the space-charge sheath as well. It follows that in the first approximation the ionization/recombination and the translational energy exchange between the electrons and the heavy particles in the sheath should be neglected. Note that in cases where one or both of parameters λ_D/d and λ_D/L_{tn} are not small, e.g., both of them are comparable to unity, the quasi-neutral description of the arc bulk, in spite of formally accounting for the ionization and thermal non-equilibria, has the same accuracy as the LTE description and should be considered as equivalent to it; the case considered in the next paragraph.

Now let us consider the case where the arc bulk plasma is described in the 2T approximation. Since terms that are small in the parameters λ_D/L and d/L are neglected in such description, the near-surface non-equilibrium layer should be introduced in the mathematical model of the arc on the whole as an infinitely thin interface separating the 2T arc bulk from the solid surface. Since the 2T approximation correctly describes deviations from thermal equilibrium only if $L_{tn} \gg d, \lambda_D$, terms that are small in the parameters d/L_{tn} and λ_D/L_{tn} must be neglected in the description of the non-equilibrium layer as well, meaning that the translational energy exchange between the electrons and the heavy particles in the non-equilibrium layer should be neglected in the first approximation. Finally, in the case where the arc bulk plasma is described in the LTE approximation, it follows from inequality (4) that the non-equilibrium layer should be introduced in the mathematical model of the arc on the whole as an infinitely thin interface separating the LTE arc bulk from the solid surface and, generally speaking, no simplifications in the non-equilibrium layer are justified.

Thus, in any self-consistent model with separate descriptions of the arc bulk and near-surface non-equilibrium layers, the computation domain for the arc bulk equations is the whole of the interelectrode gap; the near-surface non-equilibrium layers appear in the model as infinitesimally thin interfaces separating the computation domain from adjacent solid surfaces; boundary conditions for the arc bulk equations at the interfaces are obtained by solving equations describing the non-equilibrium layers; the latter equations are 1D and disregard convective transport of particles and energy, which follows from the layers being infinitesimally thin, and must conform to the approximations used in the arc bulk description as described in the preceding paragraphs.

The above reasoning does not rely on any assumptions beyond the inequalities which justify the use of the corresponding simplified description of the arc bulk plasma. Therefore, the above-described features are general and characteristic of any self-consistent model with separate descriptions of the arc bulk and near-surface non-equilibrium layers. Further simplifications of description of non-equilibrium layers are possible is special cases. In the rest of this section, we consider a special case where the length scales satisfy the hierarchy

$$\lambda_D \ll d \ll L_{tn}. \tag{8}$$

The first inequality in (8), $\lambda_D \ll d$, means that there is no ionization/recombination in the near-surface space-charge sheath. This is the case in most situations of high-pressure arc plasmas although exceptions exist; e.g., figure 2(a). The second inequality in (8), $d \ll L_{tn}$, is valid in many situations of interest as well.

In the special case (8), the condition of applicability of the 2T arc bulk description, inequality $\lambda_D, d \ll L$, amounts to the hierarchy

$$\lambda_D \ll d \ll L_{tn}, L. \tag{9}$$

The deviations from ionization equilibrium and charge separation inside the non-equilibrium layer in this special case occur on significantly different distances from the surface: of the orders of d and λ_D, respectively. Hence, the deviation from ionization equilibrium comes into play earlier, i.e., at larger distances from the surface than the deviation from quasi-neutrality. In other words, the near-surface non-equilibrium layer in the special case (9) is constituted by an ionization layer (scale of thickness d), where deviations from ionization equilibrium are localized, and a space-charge sheath (scale λ_D), positioned 'at the bottom' of the ionization layer. In the first approximation, plasma in the ionization layer should be treated as quasi-neutral and the translational energy exchange between the electrons and the heavy particles neglected. The ionization/recombination and the energy exchange should be neglected in the sheath.

The condition of applicability of the LTE arc bulk description, inequality (4), in the special case (8) amounts to the hierarchy

$$\lambda_D \ll d \ll L_{tn} \ll L. \tag{10}$$

The three kinds of non-equilibrium inside the non-equilibrium layer occur on significantly different distances from the surface. The first one to come into play, on distances of order L_{tn}, is the deviation from thermal equilibrium. Next, the deviation from ionization equilibrium comes into play on distances of order d. Finally, charge separation comes into play on distances of order λ_D. In other words, the near-surface non-equilibrium layer in this case is constituted by a layer of thermal non-equilibrium (scale of thickness L_{tn}), where deviations from thermal equilibrium are localized, the ionization layer (scale d), positioned 'at the bottom' of the layer of thermal non-equilibrium, and the space-charge sheath (scale λ_D), positioned 'at the bottom' of the ionization layer. The ionization equilibrium and quasi-neutrality hold in the layer of thermal non-equilibrium. As in the case (9) above, the plasma in the ionization layer should be treated as quasi-neutral and the translational energy exchange between the electrons and the heavy particles neglected in the first approximation; the ionization/recombination and the energy exchange should be neglected in the sheath.

2.3 Summary

In agreement with the above, one can think of four self-consistent approaches to modelling of high-pressure arc discharges and their interaction with solid surfaces: the straightforward approach, based on the unified description of the plasma in the whole interelectrode gap up to solid surfaces and described in section 2.1; and three approaches with separate descriptions of the arc bulk and near-surface non-equilibrium layers, described in section 2.2. These four approaches are summarized in table I. Here, n_S is the charged-particle density given by the condition of ionization equilibrium, so the equalities $T_e = T_h$, $n_e = n_S$, and $n_e = n_i$ designate thermal equilibrium, ionization equilibrium, and quasi-neutrality, respectively, and the corresponding inequalities designate the deviations.

Approach	Approximations and/or effects accounted for in the arc bulk	Boundary conditions at the arc-solid interfaces describe	Numerical realization
Unified modelling	$n_e \neq n_i$ $n_e \neq n_S$ $T_e \neq T_h$	Contact with the solid	Very difficult. Exists for: - 1D models; - 2D low-current arcs.
Approach with quasi-neutral description of arc bulk plasma	$n_e = n_i$ $n_e \neq n_S$ $T_e \neq T_h$	Separation of charges ($n_e \neq n_i$)	Difficult
Approach with 2T description of arc bulk plasma	$n_e = n_i$ $n_e = n_S$ $T_e \neq T_h$	Separation of charges ($n_e \neq n_i$) Ionization non-equilibrium ($n_e \neq n_S$)	Moderately difficult
Approach with LTE description of arc bulk plasma	$n_e = n_i$ $n_e = n_S$ $T_e = T_h$	Separation of charges ($n_e \neq n_i$) Ionization non-equilibrium ($n_e \neq n_S$) Thermal non-equilibrium ($T_e \neq T_h$)	Reasonably straightforward

Table I. Summary of self-consistent approaches to modelling of high-pressure arc discharges and their interaction with solid surfaces.

In approaches with separate descriptions of the arc bulk and near-surface non-equilibrium layers, the non-equilibrium layers should be introduced in the mathematical model of the arc on the whole as infinitely thin interfaces separating the arc bulk from the solid surface. Appropriate analysis of the non-equilibrium layers is needed in order to formulate boundary conditions for the arc bulk equations at these interfaces. The choice of description of the arc bulk plasma dictates the choice of the model of non-equilibrium layer. For example, if the 2T description is used for the arc bulk, then deviations from ionization equilibrium and charge separation must be taken into account in the near-surface non-equilibrium layer. One still has some freedom (e.g., deviations from ionization equilibrium and charge separation in the non-equilibrium layer may be assumed to occur in the same space region or be separated in space; ion motion in the near-cathode sheath may be assumed to be collision-free or collision-dominated), but not much.

3 State-of-the-art

If a high-pressure arc is attached to the same place on the surface of a refractory cathode for long enough (the necessary period of time depends on the power supply and may vary over a wide range, from fractions to tens of milliseconds), the surface will be heated up to temperatures of about 3000 K or higher, which are sufficient for thermionic emission. This is the so-called thermionic regime of cathode operation. Most of electric current is transported to the cathode surface by the emitted electrons, the contribution of the ions coming from the plasma is minor but non-negligible, usually of the order of 10% or higher.

In a number of important applications, the cathode is cold so that the electron emission is negligible; the non-thermionic regime of cathode operation. For example, this is the case where an arc rapidly moves along rails made of non-refractory materials such as aluminium or silver. One should hypothesize that the current is transported to such cathodes by ions diffusing from the arc bulk, a regime similar to the ion current regime of electrostatic probes. Note that this

mechanism of current transfer presumably occurs [64, 65] in spotless attachments of vacuum arcs to cathodes made of non-refractory metals, e.g., chromium or lead. (Such attachments are observed if the average cathode surface temperature is high enough, around 2,000 K for chromium and 1,200 K for lead; [66] and references therein.)

In the case of arc anodes, current is transported to the electrode surface by electrons diffusing from the arc bulk. If the temperature of the plasma in the immediate vicinity of the anode is high enough, the density of the electron diffusion current to the anode surface may exceed the current density sustained by the arc power supply. A potential barrier is built near the anode in such cases, which reflects the excess of electron current back into the plasma; the so-called negative anode voltage.

In principle, each one of the four approaches to self-consistent modelling of the near-electrode physics, summarized in table I, may be applied to all the three regimes of operation of electrodes of high-pressure arcs, described in the preceding paragraphs. In the framework of the unified modelling approach, this can be done in a straightforward way. For the other three approaches, boundary conditions on the interface separating the arc bulk from the electrode should be formulated, which correctly describe the near-electrode physics relevant for the regime under consideration. In what follows, we will consider what has been done in this direction in the literature, with an emphasis on recent publications.

3.1 Unified modelling

The unified modelling takes into account in the whole computation domain all the three kinds of deviation from LTE: a deviation from thermal equilibrium, a deviation from ionization equilibrium, and charge separation. The approach is based on using the single set of equations, including the Poisson equation, in the whole interelectrode gap up to the electrode surfaces.

The charge particle density is very high in high-pressure arc plasmas except if the arc current is very low, of the order of 1 A. The near-surface space-charge sheaths occupy only a tiny fraction of the computation domain in these conditions and the separation of charges in the bulk plasma is very small, which makes the Poisson equation stiff. Therefore, the unified approach to the modelling of high-pressure arcs is highly computationally intense and its application has been limited up to now to two situations: 1D modelling, which includes modelling of near-electrode layers of high-current arcs [13, 19, 25, 26, 67, 68] and modelling of microdischarges with low current densities [9, 34, 35], and 2D modelling of low-current arcs [7, 22, 69].

The 1D modelling of near-electrode layers of high-current arcs employs the system of differential equations that includes equations of conservation of species; equations of transport of species taking into account multicomponent diffusion and written in the form of the Stefan-Maxwell equations; the electron and heavy-particle energy equations; and the Poisson equation. The near-electrode layer is assumed to be thin, so the convective transport of particles and energy is neglected and the hydrodynamics equations are not included. Such modelling has delivered a number of useful methodological results. Let us consider, as an example, distributions of parameters in the non-equilibrium layer at a thermionic cathode of atmospheric-pressure argon arc, shown in figure 3. Here x-axis is directed from the cathode surface into the plasma, E is the x-projection of the electric field, T_w is the temperature of the cathode surface, and j_w is the density of electric current from the plasma to the cathode surface. The vertical dashed line shows the point where the deviation from the thermal non-equilibrium reaches 5%, the vertical dotted line shows the point where the deviation from the ionization non-equilibrium reaches

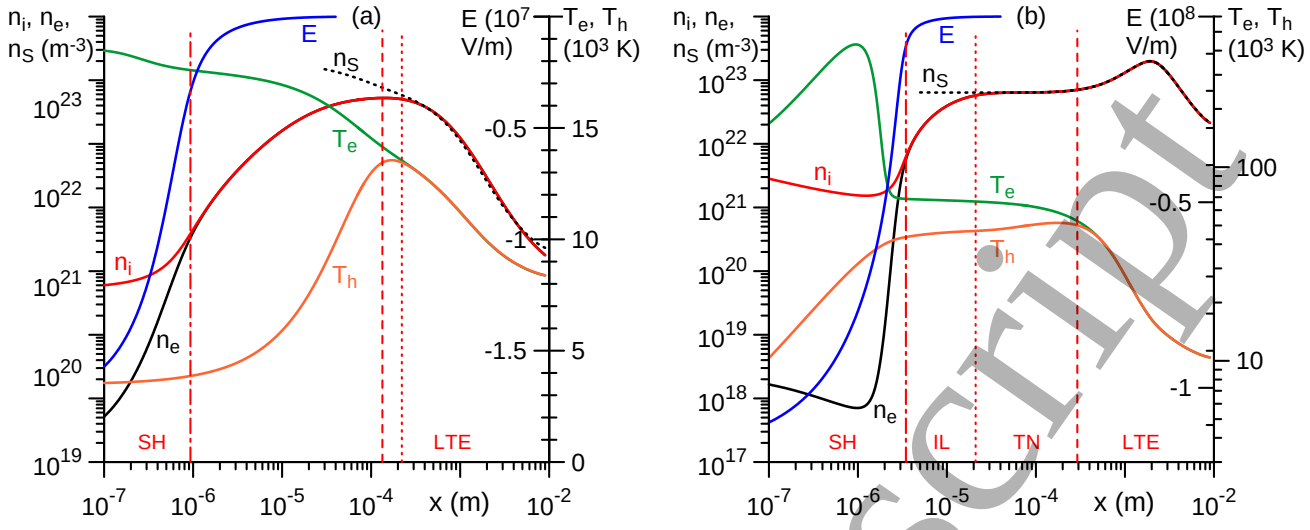

Figure 3. Distribution of parameters in the near-cathode non-equilibrium layer. Ar plasma, $p = 1$ bar, W cathode, $T_w = 3500$ K. (a): $j_w = 10^7$ A/ m^2. (b): $j_w = 7.8 \times 10^7$ A/ m^2. Adapted from [67].

10%, and the dash-dotted line shows the point where the deviation from the quasi-neutrality reaches 10%.

The structure of the non-equilibrium layer described at the end of section 2.2.3 is clearly seen in figure 3(b): the LTE region, the layer of thermal non-equilibrium (TN), the ionization layer (IL), and the space-charge sheath (SH). The LTE region and the space-charge sheath are also seen in figure 3(a), however it is not possible to distinguish between the layer of thermal non-equilibrium and the ionization layer in this figure, since the deviations from thermal and ionization equilibrium come into play in approximately the same region in space. Moreover, while the thermal equilibrium is the first one to break down for $j_w = 7.8 \times 10^7$ A m^{-2}, i.e., the vertical dashed line in figure 3(b) is located to the right of the dotted line, the ionization equilibrium for $j_w = 10^7$ A m^{-2} breaks down before the thermal equilibrium does: the vertical dotted line in figure 3(a) is located to the right of the dashed line.

It is interesting to analyze these results from the point of view of the length scales introduced in section 2.2.1. Let us designate by x_{TN}, x_{IL}, and x_{SH} the abscissas of, respectively, the vertical dashed, dotted, and dash-dotted lines in figure 3, i.e., x_{TN} is the point where the deviation from the thermal non-equilibrium reaches 5% *etc.* The numerical values are $x_{SH} = 0.9\,\mu$m, $x_{IL} = 220\,\mu$m, $x_{TN} = 130\,\mu$m for $j_w = 10^7$ A m^{-2} and $x_{SH} = 3.5\,\mu$m, $x_{IL} = 21\,\mu$m, $x_{TN} = 290\,\mu$m for $j_w = 7.8 \times 10^7$ A m^{-2}. The point $x = x_{IL}$ may be viewed as a 'boundary' of the LTE plasma region (or, equivalently, an 'edge' of the non-equilibrium layer) in the case $j_w = 10^7$ A m^{-2} and $x = x_{TN}$ plays the same role in the case $j_w = 7.8 \times 10^7$ A m^{-2}. The temperatures at these points are approximately 13, 000 and 50, 000 K, respectively. The Debye length λ_D, the ionization length d, and the length of temperature relaxation L_{tn}, shown in figure 1(b), are $\lambda_D = 0.02\,\mu$m, $d = 220\,\mu$m, $L_{tn} = 110\,\mu$m for $T_h = T_e = 13,000$ K and $\lambda_D = 0.06\,\mu$m, $d = 13\,\mu$m, $L_{tn} = 250\,\mu$m for $T_h = T_e = 50,000$ K.

One can see that the estimates of d and L_{tn} give a correct idea of the orders of magnitude of x_{IL} and x_{TN}. In particular, they explain why the thermal equilibrium is the first one to break down for $j_w = 7.8 \times 10^7$ A m^{-2} and the ionization equilibrium is the first one to break down for $j_w = 10^7$ A m^{-2}.

On the other hand, λ_D is lower than x_{SH} by more than an order of magnitude. This dis-

crepancy is unsurprising, since the charged particle density at the 'edge' of the non-equilibrium layer, used in the above evaluation of λ_D, is much higher than that at the sheath 'edge', and the sheath voltage is much higher than kT_e. (Note that values of the Debye length estimated in terms of the charged particle density at $x = x_{SH}$ and of the sheath voltage instead of kT_e are $0.4\,\mu$m for $j_w = 10^7\,\mathrm{A\,m^{-2}}$ and $1.4\,\mu$m for $j_w = 7.8 \times 10^7\,\mathrm{A\,m^{-2}}$, i.e., give the correct order of magnitude of x_{SH}.) This is an example of limitations of the qualitative analysis of section 2.2, which, of course, must exist given the simplicity of the length scale estimates on which the analysis is based.

Another result of the unified modelling of the near-cathode regions [67] is that the energy flux in typical situations is directed not from the bulk plasma to the near-cathode layer, but from the layer into the bulk. In other words, it is the near-cathode layer that heats the arc bulk rather than the other way round. This is a consequence of a significant power deposited by the arc power supply into the near-cathode non-equilibrium layer, mostly into the space-charge sheath. A part of this power is transported to the cathode surface, thus heating it to temperatures sufficient for electron emission, and the rest is transported into the arc bulk plasma in the form of enthalpy flux carried by the electron current.

The unified 1D modelling of near-anode layers in arc discharges in several gases (Ar, Xe, and Hg) in a wide range of conditions was reported in [19] and the results were interpreted in terms of the anode heating voltage. In [25, 26], the unified 1D modelling of short argon arcs with hot anode was reported, which are of interest in connection with production of carbon nanoparticles. In [25], the numerical model was formulated and validated against previous simulation results [67] and experimental data. It was found that the anode voltage is negative and depends on the anode cooling intensity. In [26], an analytical model of the whole arc was developed, comprising models for near-electrode regions and the arc column. The model was validated against experimental data and verified by comparison with numerical solution.

The unified 1D modelling of transition from glow to arc regimes in microdischarges in atmospheric-pressure argon was reported in [9, 34]. Detailed plasma chemistry was taken into account. The inter-electrode gap was $39\,\mu$m in [9] and $400\,\mu$m in [34]. The dynamics of arc discharge formation was studied in [9] and it was shown that the discharge takes the form of glow immediately after the breakdown, and then, when the cathode surface temperature becomes sufficiently high, transits to stable arc discharge; an understandable result. The effect of different variants of the drift–diffusion description of the electron transport was investigated in [34] and it was shown that it can affect spatial distributions of the particle densities and temperatures. The work [35] continues the study started in [34]; further details are given and the modelling is extended into the range of higher current densities, from $10^6\,\mathrm{A/m^2}$ to $2.3 \times 10^6\,\mathrm{A/m^2}$, where the discharge operates as a microarc.

The unified 2D modelling of axially symmetric low-current discharges in atmospheric-pressure argon in a cylindrical tube was reported in [22, 69] for discharge currents of up to about 30 mA and in [7] for currents up to 2 A. (In [22, 69], simulation results are reported also for a plane gliding-arc geometry.) The equations of transport of the charged particles are written in the drift-diffusion approximation without account of the multicomponent diffusion, which is consistent with low discharge currents being considered and, consequently, low ionization degree of the plasma. The pioneer works [7, 22, 69] gave interesting results. In particular, the arc drag by the gas and the arc gliding along the electrodes was studied qualitatively in [69]. A transition from glow to arc discharge was simulated in [7] and it was found that the cathode surface is heated to about 3500 K in fractions of millisecond (at the power supply voltage of 10 kV) due to ion bombardment and, to a lesser degree, to heat flux from the discharge gap. It is interesting

to note that although the modelling conditions in [7, 22, 69] are apparently not very different, the electron number densities reported in these works differ by orders of magnitude: in excess of $10^{21}\,\mathrm{m}^{-3}$ in [22, 69] and of the order of $10^{16}\,\mathrm{m}^{-3}$ in [7].

3.2 Approach with quasi-neutral description of the arc bulk

There is a number of works where the whole interelectrode gap is described with account of ionization and thermal non-equilibrium under the assumption of quasi-neutrality, i.e., near-surface space-charge sheaths are discarded, e.g., [56–63]. The physics of this approach is problematic, especially as far as the arc-cathode interaction is concerned (in particular, there are difficulties with the electric current and energy balance; e.g., discussion in [70, 71]). One of the consequences is that an artificial restriction of the current-collecting part of the cathode surface is needed in some models in order to obtain a current density distribution concentrated at the cathode tip, which is necessary to reproduce the thermionic behavior in the arc root; e.g., discussion in [20]. Therefore, it is imperative to introduce an account of near-surface space-charge sheaths, in the first place, the near-cathode sheath.

As discussed in section 2.2, if the arc bulk is described under the assumption of quasi-neutrality with account of ionization and thermal non-equilibrium, then the near-surface non-equilibrium layers represent space-charge sheaths and should be introduced as infinitely thin interfaces separating the bulk plasma from solid surfaces. Boundary conditions at these interfaces for the quasi-neutral arc bulk equations have to be obtained by means of solving the sheath equations and matching the solution to a solution of the quasi-neutral equations. The ionization/recombination and the translational energy exchange between the electrons and the heavy particles should be neglected in the first approximation and the sheath equations are not too difficult to solve. The matching, on the other hand, is not easy. The standard procedure which allows one to derive self-consistent and unique boundary conditions is asymptotic matching. However, such procedure would be too complex in this case: space-charge sheaths are assumed to be collisionless in most works, and a solution describing a collisionless sheath cannot be matched directly with a solution describing the collision-dominated quasi-neutral bulk, hence an intermediate region (the Knudsen layer) would have to be treated. It is unsurprising therefore that different boundary conditions have been used, including the much-criticized so-called collision-dominated Bohm criterion [23, 72, 73]; other examples can be found in [31, 32, 74].

In [6], boundary conditions describing positive and negative near-surface space-charge sheaths in high-pressure arc discharges were derived by means of a procedure which aimed to be as close to asymptotic matching as possible, while still being practicable. In [8], the boundary conditions derived in [6] have been implemented in the 2D model of the arc and the developed model was applied for investigation of thermal and chemical non-equilibrium in conditions of experiment with a free-burning atmospheric-pressure argon arc [75]. For the sake of stability and low computational cost, the simulations have been performed assuming the anodic sheath voltage equal to zero. For all current levels, a field reversal in front of the anode accompanied by a voltage drop of $0.7 - 2.6\,\mathrm{V}$ was observed. Another field reversal was observed near the cathode for arc currents below 80 A. This study was continued in [10]. Results of modelling of atmospheric-pressure argon arcs burning between a doped tungsten cathode with a truncated conical tip and a water-cooled anode made of copper in the arc current range $100 - 200\,\mathrm{A}$ were reported in [20]. In particular, it was concluded that differences of the order of a few per cent appeared when the number of excited states was increased beyond the first one, but the computational effort grew very rapidly.

In [28], a 3D transient model with the arc bulk described with account of ionization and thermal non-equilibrium under the assumption of quasi-neutrality was applied to simulation of atmospheric-pressure argon arc between a thoriated-tungsten cathode and a coaxial tubular copper anode at the arc current of 700 A. Multiply charged ions (Ar^+, Ar^{2+}, Ar^{3+}) have been taken into account. The cathode sheath model was based on an 'effective' value of plasma conductivity inside cathode boundary cells, which was determined with account of different physical process in the sheath. Anode sheath was not considered. This study was continued in [33] for the 2D steady-state case and arc current equal to 100 or 200 A. It was concluded that the 1D sheath treatment using the effective value of sheath electrical conductivity is helpful in obtaining more realistic numerical results than those without sheath treatment.

1D numerical modelling of ablating atmospheric-pressure carbon arcs, which are employed for the synthesis of carbon nanomaterials, was reported in [32]. Detailed carbon chemistry was taken into account and the species considered were atomic, diatomic, and triatomic carbon in ground, excited, and ionized states (C, C_2, C_3, C^*, C_2^*, C_3^*, C^+, C_2^+, C_3^+), helium as the buffer gas, and electrons. The quasi-neutral bulk plasma model was coupled with sheath models at the electrodes.

3.3 Decoupling of the cathodic part of arc on thermionic cathode and the concept of anode heating voltage

Now it is convenient to consider two approximations that are often used in the analysis of current transfer to electrodes of high-pressure arc discharges: decoupling of the cathodic part of the arc and the approximation based on the concept of anode heating voltage. The unified modelling approach and the approach with quasi-neutral description of the arc bulk, reviewed in the previous sections, do not employ these approximations and, consequently, can be used in order to justify these approximations and determine conditions of their applicability. On the other hand, these approximations are relevant to approaches with 2T and LTE descriptions of the arc bulk, reviewed in sections 3.4 and 3.5 below.

3.3.1 Decoupling of the cathodic part of arc on thermionic cathode

Simple estimates (e.g., [70]) show that a contribution of the energy flux from the arc bulk to the energy balance of the non-equilibrium layer at a thermionic cathode is minor and hence the energy flux coming from the near-cathode layer to the cathode surface is generated inside the layer. (Of course, this does not apply to cases where the plasma-cathode interaction is dominated by arc-related phenomena, such as plasma jets impinging on the cathode surface.) Note that a simplified version of this hypothesis can be found already in the 1963 publication [76]: 'the power brought into the ion production zone by the electron beam emerging from the space charge layer is all consumed in producing the ions which flow to the cathode'. Later, this hypothesis was confirmed by the unified modelling of the near-cathode non-equilibrium layers [67]: as mentioned in section 3.1, it was shown that there is a significant power deposited by the arc power supply into the near-cathode non-equilibrium layer and a part of this power is transported to the cathode surface and heats the surface to temperatures sufficient for electron emission, while the rest is transported into the arc bulk in the form of enthalpy flux carried by the electron current. (It is interesting to note that in cases where the current transfer occurs in the spot mode, the power transported into the bulk significantly exceeds the power transported to the cathode [77].)

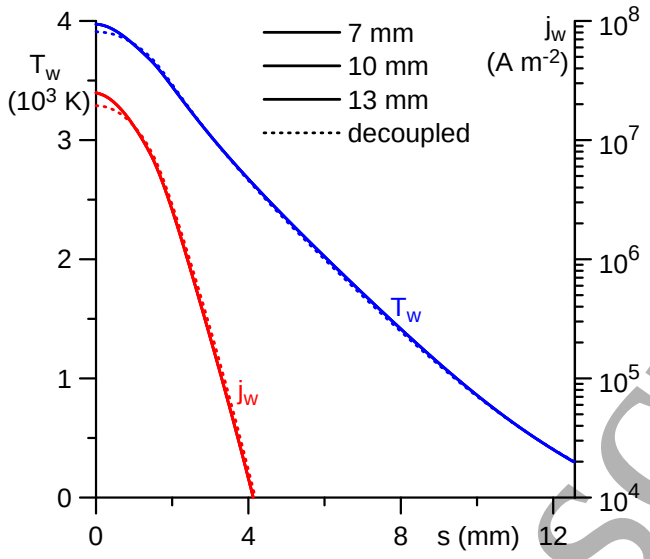

Figure 4. Distributions along the cathode surface of the surface temperature T_w and the electric current density j_w. Free-burning Ar arc, $p = 1$ bar, $I = 100$ A. Solid: computation by means of the approach with the quasi-neutral description of the arc bulk for three different values of the interelectrode distance: 7, 10, and 13 mm. Dotted: decoupled calculation of the cathodic part of the arc with the use of the model [70, 78, 79]. From [6].

Moreover, it is natural to hypothesize that the voltage drop across the near-cathode layer does not vary appreciably inside the arc attachment. Citing [76] again: 'The cathode fall voltage is taken to be independent of position over the emitting region, since it is the potential difference between two good electrical conductors, the cathode and the plasma'.

A consequence is that the cathodic part (the cathode and the near-cathode non-equilibrium layer) of a high-pressure arc discharge with a thermionic cathode is governed primarily by processes in the near-cathode layer; the effect of processes in the arc bulk is weak. An illustrative example is shown in figure 4. The figure refers to a free-burning atmospheric-pressure argon arc with a tungsten cathode in the form of a rod with a hemispherical tip, a length 12 mm, and a radius 1 mm; the anode is planar and made of copper. The solid lines in figure 4 depict distributions along the cathode surface of the temperature and the current density, computed by means of the approach with the quasi-neutral description of the arc bulk, described in section 3.2, for the arc current $I = 100$ A and three different values of the interelectrode distance: 7, 10, and 13 mm. The distance s is measured from the centre of the front surface of the cathode along the generatrix of the cathode surface, so $s = 0$ corresponds to the centre of the front surface and $s = 12.57$ mm corresponds to the cathode base, which is maintained at 300 K. The three lines corresponding to the different interelectrode distances coincide: parameters of the cathodic part of the arc are independent of the arc length. This supports the above-described conclusion that the cathodic part of a high-pressure arc with thermionic cathode is governed primarily by processes in the near-cathode layer and is virtually independent of processes in the arc bulk. Note that it could be of interest to simulate in the future also shorter arcs: the minimal gap length for which the cathodic part is not affected would give an indication of thickness of the near-cathode layer.

It follows that the cathodic part of a high-pressure arc discharge to the first approximation may be computed independently of the arc bulk. This is done in two steps. First, one

solves one-dimensional equations describing the near-cathode non-equilibrium layer and finds all parameters of the near-cathode layer, in particular, the densities of energy flux and electric current from the plasma to the cathode surface, as functions of the local cathode surface temperature T_w and the near-cathode voltage drop U: $q_w = q_w(T_w, U)$, $j_w = j_w(T_w, U)$. At the second step, one solves the multidimensional heat conduction equation in the cathode body, the relation $q = q(T_w, U)$ playing the role of a boundary condition at the surface. After this problem has been solved, one will know distributions along the surface of the temperature and, consequently, all the other parameters and also the arc current, corresponding to the U value considered. Then the problem is solved for another U value *etc.*

A very important feature of this approach is the existence under certain conditions of more than one solution at the same value of the arc current. These solutions describe different modes of current transfer to the cathode: the diffuse (spotless) mode and modes with one or more cathode spots in different configurations. This feature allows for a self-consistent calculation of different modes of arc attachment to the cathode, thus eliminating the necessity of switching different mechanisms (such as thermionic electron emission versus thermo-field or field emission) 'by hand' in order to obtain different modes, which is the usual way of simulating different modes in other models. In essence, the existence of different modes of current transfer in the framework of this approach is a manifestation of non-uniqueness of thermal balance of a finite body heated by an external energy flux depending in a nonlinear way on the local surface temperature. For this reason, this approach is sometimes called the model of nonlinear surface heating. Note that these multiple solutions fit the general pattern of self-organization in bistable nonlinear dissipative systems, which allows to understand these solution within a physically transparent framework without going into mathematical details and also facilitates a systematic computation of these solutions [80].

The approach based on decoupling of calculation of cathodic part from the rest of the arc was apparently proposed for the first time by Bade and Yos [76] and was re-discovered more than once; see [42] for references and discussion. By now this approach has gone through a detailed experimental validation for low-current arc discharges. One can specifically mention works of Mentel and coworkers, in particular, [81]; further examples of experimental verification and references can be found in [42, 82–84]. One can mention also works [85], where a self-organized pattern of several cathode spots, predicted by the model of nonlinear surface heating, was observed in experiments with a magnetically rotating arc, and [86], where the model of nonlinear surface heating was used to simulate the change in shape of thermionic cathodes occurring during the arc operation at currents in the range $60 - 150$ A and produced results in a quite good agreement with the experiment.

A realization of the approach based on decoupling of calculation of cathodic part from the rest of the arc requires a model of near-cathode non-equilibrium layer to be employed. Such model may be based on the universal description of the near-cathode layer, discussed in section 3.1. As an example, characteristics of the cathodic part of an atmospheric-pressure argon arc, computed in the framework of the decoupling approach with the use of use of the unified modelling code [67], are shown in figure 5 by solid lines. (Here U_{sh} is the sheath voltage and $T_e^{(il)}$ is the average electron temperature in the ionization layer.) In this example, the lateral surface of the cathode was assumed to be thermally and electrically insulated, so the energy flux and the electric current from the plasma enter the cathode through the front surface and leave it through the base (which is maintained at 300 K); the solution of the heat conduction equation in the cathode body is 1D (the temperature varies only in the axial direction) and all parameters, including T_w and j_w, do not vary along the cathode surface.

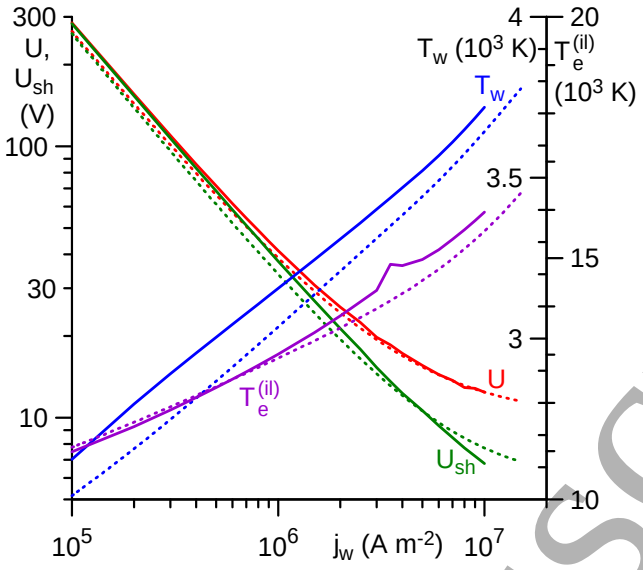

Figure 5. Parameters of the cathodic part of the arc computed by means of the decoupling approach. Solid: calculations with the use of the unified modelling code [67]. Dotted: Internet tool [87]. Ar plasma, $p = 1$ bar, 1 cm-height W cathode, temperature at the cathode base 300 K. Adapted from [6].

An alternative to the unified modelling of the near-cathode non-equilibrium layer is an approach based on dividing the non-equilibrium layer into sub-layers where different physical mechanisms are dominant. The most important are sublayers where the energy flux to the cathode surface is formed: the ionization layer, where the ion flux to the cathode surface is generated, and the space-charge sheath, where the emitted electrons are accelerated by the sheath electric field, thus gaining energy for ionization of neutral atoms, and the ions are accelerated in the direction to the cathode.

As an example, results of the decoupled calculation of the cathodic part of the arc with the use of the model of ionization layer and space-charge sheath [70, 78, 79] are shown by the dotted lines in figure 4. One can see that these results are in excellent agreement with those given by the approach with the quasi-neutral description of the arc bulk, which does not rely on decoupling of the cathodic part from the rest of the arc and is significantly more laborious. Another example is shown in figure 5, where the dotted lines represent results obtained with the use of the model of ionization layer and space-charge sheath [70, 78, 79]. These results are in very good agreement with those given by the unified modelling, which is again significantly more laborious.

Simulation of interaction of high-pressure arcs with thermionic cathodes by means of the decoupling approach is relatively easy and has become a matter of routine. In particular, a free on-line tool for simulation of current transfer to rod cathodes is available in the Internet [87]. The tool employs the model of ionization layer and space-charge sheath [70, 78, 79]. The database of plasma-producing gases includes, but is not limited to, He, Ne, Na, Ar, Cu, Kr, Xe, Cs, Hg, air, mixtures Na-Hg and Cs-Hg, plasmas of mercury or xenon with addition of metal halides. The database of cathode materials includes, but is not limited to, W, Mo, Hf, Fe, Nb, Zr. The tool simulates the diffuse mode of arc attachment, the first axially symmetric spot mode (i.e., a mode with a spot at the center of the front surface of the cathode), and bifurcation points positioned on the diffuse mode, including the first bifurcation point that represents the limit of stability of the diffuse mode.

Note that the results depicted by the dotted lines in figure 5 have been obtain by means of this tool. While the tool is capable of computing both the diffuse and spot modes of current transfer, the results in figure 5 refer to the diffuse mode, where the temperature in the cathode varies only in the axial direction.

3.3.2 Anode heating voltage

There is a fundamental difference between the physics of current transfer to anodes and thermionic cathodes of high-pressure arc discharges; e.g., discussion in section 2 of [42]. In particular, while a significant power is deposited by the arc power supply into the near-cathode non-equilibrium layer, mostly into the space-charge sheath, the power deposited into the near-anode layer is not significant and may be even negative. Therefore, the decoupling approach discussed in the previous section, while being applicable to cathodes, does not apply to anodes.

Another popular tool for approximate analysis of plasma-electrode interaction in high-pressure arc discharges is the concept of volt equivalent of the heat flux to electrode; e.g., [88] and references therein and [89] as a more recent example. This concept is based on the assumption that the density of the energy flux from the plasma to the electrode is proportional to the local current density:

$$q_w = j_w U_h, \tag{11}$$

where the proportionality coefficient U_h (the electrode heating voltage, or volt equivalent of the heat flux to the electrode) may depend on the plasma-producing gas and its pressure and on the electrode material. If U_h is known, one can estimate the integral power input from the plasma to the electrode, Q, for any given arc current I: $Q = IU_h$.

The concept of electrode heating voltage is not applicable to cathodes: there is no proportionality between the energy flux from the arc to a cathode and the arc current in any meaningful sense. However, it represents a good approximation for anodes. A theoretical confirmation of the latter was given, in particular, by the unified numerical modelling of near-anode layers in arc discharges in several gases (Ar, Xe, and Hg) in a wide range of current densities (up to $10^7\,\mathrm{A\,m^{-2}}$), anode surface temperatures ($300 - 3000\,\mathrm{K}$), and plasma pressures ($1 - 100\,\mathrm{bar}$) [19]. It was shown that the density of energy flux to the anode is virtually independent of the anode surface temperature and varies approximately linearly with the current density; a result that represents a theoretical justification of the concept of anode heating voltage. Values of the anode heating voltage for the above conditions are reported.

The assumption (11) (or, more precisely, the relation $Q = IU_h$) for the case of anode is supported also by experimental data. In particular, the experiments [90], performed with tungsten rod electrodes of different dimensions in a 2.6 bar Ar arc, are well described by this relation with $U_h = 6.24\,\mathrm{V}$ [91]. The latter value is close to 6.1 V, which is the value obtained by the linear interpolation over p of the corresponding data in table 1 of [19]. A similar linear behavior was found for a tungsten anode operating in a xenon plasma under the pressure of about 100 bar [68], with U_h about 5.4 V. Again, this is close to the corresponding computed value given in table 1 of [19] (5.9 V).

Thus, the concept of volt equivalent of the heat flux to electrode conforms to both experiment and the modelling in the case of anodes. Note that a similar concept, with the arc being described by means of electrical circuit analogy, is used in welding, although for a different purpose; e.g. [92].

3.4 Approach with 2T description of the arc bulk

As discussed in section 2.2.3, if the arc bulk plasma is described in the 2T approximation, which takes into account thermal non-equilibrium but still assumes the ionization equilibrium and quasi-neutrality, then the model of the near-surface non-equilibrium layers should take into account a deviation from the ionization equilibrium and the charge separation; the translational energy exchange between the electrons and the heavy particles in the non-equilibrium layers should be neglected in the first approximation. In principle, such model may employ a unified modelling of the non-equilibrium layers, similar to the 1D modelling of near-electrode layers described in section 3.1 but with the translational energy exchange terms dropped. An alternative is to divide the non-equilibrium layer into a quasi-neutral ionization layer and a space-charge sheath with frozen ionization and recombination, as described in section 2.2.3 (the paragraph after equation (9)). The former (unified-modelling) approach apparently has not been pursued in the literature. In contrast, models considering, in some or other way, the ionization layer and space-charge sheath at thermionic cathodes have a long history; see section 3.2.1 of [42] for references and discussion.

One of such models was developed in [70, 78, 79]. The model employs the assumption that the energy flux coming from the near-cathode layer to the cathode surface is generated inside the layer, which has already been discussed in section 3.3.1 and is one of the assumptions allowing decoupling of the cathodic part of the arc from the arc bulk. A summary of equations of the model is given in [93]. A free tool for computation of integral characteristics of the non-equilibrium near-cathode layer, based on this model, is available on Internet [94].

Let us return to figure 5, where results obtained by means of the model [70, 78, 79] are compared with those given by the unified modelling. This example shows that the 'ionization layer - space-charge sheath' approach is capable of describing integral characteristics of non-equilibrium layers on thermionic cathodes with surprising accuracy. Note that the electron temperature does not vary dramatically across the near-cathode layer in some cases; e.g., figure 3(a). In other cases, there is a very large variation of T_e in the space-charge sheath, which is due to a strong heating of the emitted electrons by the sheath electric field, however, the variation of T_e in the ionization layer remains relatively small; e.g., figure 3(b). This explains why the integral-balance evaluation of the average electron temperature in the ionization layer, employed in the model [70, 78, 79], is accurate over the whole range of j_w shown in figure 5. Further discussion of this point can be found in [6].

Modelling of the arc on the whole by means of 2T arc bulk equations supplemented with boundary conditions describing the non-equilibrium layer at thermionic cathodes was reported in [14, 17, 21, 71, 95]. The treatment [71, 95] employed the 'ionization layer - space-charge sheath' model [70, 78, 79]. The boundary conditions for the electron and heavy-particle temperatures in the bulk, $T_e^{(pl)}$ and $T_h^{(pl)}$, at the arc-cathode interface were conditions of continuity, meaning that $T_e^{(pl)}$ at the interface equals $T_e^{(il)}$ the electron temperature in the ionization layer, which is governed by the balance of the electron energy in the ionization layer, and $T_h^{(pl)}$ at the interface equals T_w the temperature of the cathode surface. It should be stressed that this way of matching of the 2T bulk and the non-equilibrium near-cathode layer is in line with analysis of section 2.2.3 and follows from asymptotic matching. In order to simplify the workflow, the voltage drop in the near-cathode layer was assumed to be the same at all points inside the arc attachment. Under this assumption, the equations describing the cathodic part of the arc became independent from the rest of the equations and were solved independently, which amounts to the decoupling of the cathodic part, discussed in section 3.3.1. The distribu-

tions of the cathode surface temperature, the electron temperature in the ionization layer, and the current density, computed as a part of the cathodic-part solution, served as the boundary conditions at the arc-cathode interface for the 2T equations, which were solved at the second step.

The effect of the arc bulk over the cathodic part, neglected in [71, 95], is two-fold. First, there is an electrical coupling: the electrical resistance of the bulk can cause a variation of the near-cathode voltage drop inside the arc attachment. Second, there is a thermal coupling: the energy exchange between the near-cathode plasma and the bulk can affect the energy flux to the cathode. The electric coupling is not very important: numerical results [71] have shown that the potential distribution given by the arc bulk modelling varies little inside the arc attachment, by no more than approximately 1 V. In any case, an account of the electric coupling in numerical modelling does not require the model to be changed; it is just a matter of changing the workflow: iterations between the cathodic part and the arc bulk will be needed.

The thermal coupling is not very important inside the cathodic arc attachment, where the current density is high. However, it may become important outside the arc attachment. It follows that the model [71, 95] is accurate in cases where heat exchange of the cathode with the adjacent gas outside the arc attachment does not contribute appreciably to the heat balance of the cathode. The model may become insufficient in other cases, e.g., if cold gas is pumped along the cathode surface. Thus, a description of the thermal coupling of the cathode with the arc bulk may be needed.

The electrical and thermal coupling of the cathode with the arc bulk was studied in [14, 17, 21]. One of the modification introduced in [14, 17, 21] in order to describe the thermal coupling effect was as follows: an additional region termed thermal perturbation layer was introduced, where ionization equilibrium does not hold and the charged particle density is governed by a 2D equation written with account of ambipolar diffusion, convective transport, and ionization/recombination. In effect, the authors [14, 17, 21] relaxed the assumption that the ionization layer is thin and can therefore be described in the 1D approximation, employed in the 'ionization layer - space-charge sheath' model [70, 78, 79], and divided this layer into two parts: the outer part, which is described by a 2D ambipolar diffusion equation with convection, and the 1D Knudsen layer, where a solution with account of ion inertia is used. It is not clear what boundary conditions have been used in order to ensure matching of solutions in the arc bulk and the thermal perturbation layer; note that it is problematic from the theoretical point of view to consider two adjacent regions assuming that ionization/recombination dominates over the convective transport of the charged particles in one region (the bulk) and is comparable to the convective transport in the other (the thermal perturbation layer). Apparently, further work on this topic is needed.

A useful improvement would be to introduce, in the framework of the 2T equations describing the arc bulk, the account of diffusion current in Ohm's law, as mentioned in section 2.2.2. Representative modelling results [49] showed that the new form of Ohm's law, when introduced into standard LTE or 2T models, may describe the electric field reversal in front of arc anodes, an effect that has been simulated previously only by means of (more complex) models taking into account deviations from ionization equilibrium.

3.5 Approach with LTE description of arc bulk plasma

The approach combining the LTE description of the arc bulk with some or other model of deviations from LTE occurring near solid surfaces was reviewed very recently by Choquet [36],

mainly in connection with the modelling of the welding arcs (one can mention also subsequent publications [18, 31]), therefore a discussion here is very brief.

As discussed in section 2.2.3, if the arc bulk plasma is described in the LTE approximation, then the model of near-surface non-equilibrium layers should take into account all the three kinds of non-equilibrium: a deviation from thermal equilibrium, a deviation from ionization equilibrium, and charge separation. Such model may employ a unified modelling of the non-equilibrium layers, an example being shown by the solid lines in figure 5. An alternative is to divide the non-equilibrium layer into the layer of thermal non-equilibrium, the ionization layer, and the space-charge sheath, as described at the end of section 2.2.3. In this spirit, in [18] the LTE description of the arc bulk was combined with the 'ionization layer - space-charge sheath' model [70, 78, 79]. The layer of thermal non-equilibrium, however, was discarded. Plasma-anode interaction was described by means of the concept of anode heating voltage, discussed in section 3.3.2. As in the model with the 2T description of the arc bulk [71, 95], the voltage drop in the near-cathode layer was assumed to be constant inside the arc attachment, which allowed to compute the cathodic part of the discharge and the LTE arc bulk successively without iterations.

The effect of the electric coupling of the cathodic part with the LTE arc bulk was studied in [96] and found minor. On the other hand, an account of the thermal coupling may be useful, similarly to what was said in the preceding section. This may require the account of the layer of thermal non-equilibrium. Also useful can be another modification, which was mentioned in the preceding section as well, namely, the introduction, in the framework of the LTE equations describing the arc bulk, of the diffusion current in Ohm's law [49].

4 Comparison of results obtained using various non-equilibriu approaches and the relationship with the conventional LTE models

In figure 6, current-voltage characteristics (CVCs) of a free-burning argon arc, given by three of the self-consistent approaches summarized in table I, namely, the approaches with the quasi-neutral, or 2T, or LTE descriptions of the arc bulk plasma, are shown along with the experiment. One can see that the arc voltages given by the three approaches agree with each other and with the experiment reasonably well in the whole arc current range $20 - 175$ A.

Also shown in figure 6 is the CVC evaluated in the framework of the conventional LTE model, i.e., without account of near-electrode non-equilibrium layers. This CVC is of a different character than the ones given by all the non-equilibrium models and the experiment: the arc voltage monotonically increases for all currents. This difference stems from the neglect of the near-electrode layers in the conventional LTE model, rather than from the mere fact that deviations from LTE become more pronounced as the arc current decreases.

Further examples of comparison of results given for the same conditions by different non-equilibrium approaches can be found in [6, 18, 20, 25, 97]. Note that it was pointed out in [2] (figure 6 [2]) that the temperatures in the argon arc column within a few millimeters of the cathode predicted in [71, 97] for $I = 160$ A, which attain approximately $14,000$ K, are lower than values given by the laser-scattering measurements [98] for $I = 150$ A, which go up to approximately $19,000$ K. One should keep in mind, however, that while the measurements [98] have been performed with a thoriated-tungsten cathode of diameter 3.2 mm that was sharpened

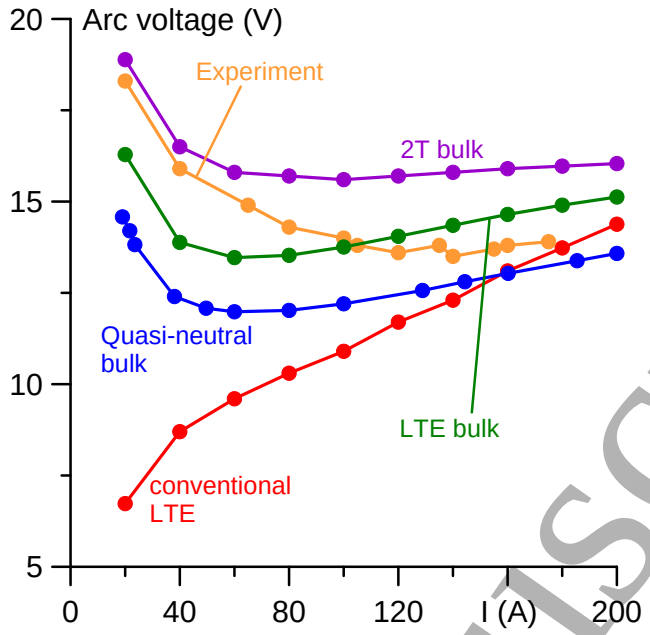

Figure 6. Arc voltage evaluated by means of different models and the experimental data. Ar arc, $p = 1$ bar, rod hemispherically-tipped tungsten cathode of length of 12 mm and radius of 1 mm, planar copper anode, the interelectrode gap 10 mm. Quasi-neutral bulk: [8]. 2T bulk: [71]. LTE bulk: [18]. Experiment: [75]. Conventional LTE: [71]. From [18].

to a conical tip with an included angle of 60°, the modelling [71, 97] refers to a pure-tungsten cathode of radius 1 mm with a hemispherical tip. One should presume that it is this difference that results in the different arc column temperatures. Indeed, simulations for a conical cathode [18, 20] gave significantly higher temperatures than those reported in [71, 97]: in excess of 20, 000 K.

Moreover, the modelling [18] has predicted a strong effect produced by details of the cathode geometry over the distribution of the current density along the cathode surface and therefore over the arc plasma temperature; an interesting and potentially important effect. In particular, this effect should be kept in mind in comparison of modelling and experiment.

In spite of the advances achieved in the modelling of deviations from LTE occurring near electrodes, reviewed in the preceding sections, the conventional LTE models (i.e., MHD models based on the assumption of LTE in the whole plasma computation domain up to the electrode surfaces and neglecting all deviations from LTE occurring near electrodes) remain the most widely used tool of high-pressure arc simulations, especially under conditions of industrial interest. While many works were restricted to modelling of the arc (and the cold gas) leaving aside the electrodes and assuming a given distribution of the temperature and current density along the electrode surfaces, the unified modelling of arcs and their electrodes with the LTE description of the plasma domain, introduced in [99, 100], has become mainstream. In particular, LTE models coupled with simulations of melting of electrodes made of non-refractory metals (e.g., steel) and of motion of the melt are state of the art in studies of gas metal arc welding (GMAW) and plasma cutting; e.g., reviews [2, 101].

One of issues to be dealt with in the models with the LTE description of the whole plasma domain is the fact that the electrical resistance of the near-electrode plasma is overestimated by orders of magnitude if evaluated in the LTE approximation, which results in unrealistically

high values of the near-electrode voltage drop, in excess of 1 kV; e.g., discussion in [71]. The only way to resolve this issue without taking into account the deviations from LTE occurring near electrodes is to perform a numerical cut-off. For instance, it is frequently assumed that the plasma conductivity inside each numerical cell adjacent to an electrode surface is constant and equal to the value corresponding to the temperature at the outer boundary of the cell (the boundary on the bulk-plasma side). The size of the numerical cells adjacent to electrode surfaces should be not too small for such cut-off to work, typically no less than 100 μm.

LTE models of high-pressure arc discharges built along these lines predict arc voltages which are close to experimental values for currents typical of welding arcs (of the order of 200 A). However, the same numerical cut-off could hardly produce accurate results in a wide range of conditions, and this is clearly seen in figure 6: the LTE model predicts a different variation of the arc voltage with I. The quantitative difference, while being appreciable for currents below 120 A, does not exceed approximately 2 V for $I \gtrsim 120$ A, however the latter does not prove the physical validity of the LTE description in this current range: about two thirds of the arc voltage is contributed by the near-cathode sheath, which is discarded in the LTE description. The LTE model overestimates the resistance of the part of the column that is adjacent to the cathode, as shown in [71] and mentioned above, and in certain conditions this overestimation may compensate the neglect of the voltage drop in the near-cathode sheath.

Another issue of LTE models of high-pressure arc discharges, equally well known, is related to the evaluation of the energy flux coming to the electrode surface from the plasma. It is usually set equal to the sum of the thermal-conduction flux evaluated in the LTE approximation and an additional heat flux, q_{add}, which is different for the anode and the cathode. In the case of the anode, this additional heat flux is usually attributed to electron condensation:

$$q_{add} = j_w A_f / e, \tag{12}$$

where A_f is the work function of the electrode material.

The case of the cathode is admittedly more controversial [2]. The most clear description of the approach used in this case is given in [2] and may be expressed as follows:

$$q_{add} = j_i A_i / e \tag{13}$$

with $j_i = j_w - j_R$ for thermionic cathodes and

$$q_{add} = j_i \left(U - A_f/e\right) \tag{14}$$

with $j_i = j_w$ for non-thermionic cathodes. Here j_i has the meaning of the density of ion current from the plasma to the cathode, A_i is the ionization potential of the plasma-producing gas, U is the measured cathode sheath voltage, which is assumed to be of the order of 15 V for most metals, and j_R is the electron thermionic emission current density evaluated by means of Richardson's equation.

Equations (12) and (14) resemble the concept of electrode heating voltage, discussed in section 3.3.2, with the heating voltage equal to A_f/e and $U - A_f/e$, respectively. The value of A_f/e (4.5 V for copper) is somewhat lower than the typical value of the anode heating voltage mentioned in section 3.3.2, however these two values do not look inconsistent since the heating voltage of section 3.3.2 refers to the total heat flux coming from the plasma to the anode surface. It is interesting to note that the standard 2T model without account of non-equilibrium near-electrode layers allowed modelling self-organized spot patterns on the anode of a free-burning

arc in atmospheric-pressure argon [47, 48], which is impossible to do for thermionic cathodes without proper account of the non-equilibrium layer.

The right-hand side of equation (14) lacks the term $j_i A_i/e$, which is present in equation (13). On the other hand, one can view U as an 'effective' value, ensuring agreement with the experiment. In any case, no self-consistent numerical modelling of operation of non-thermionic cathodes of high-pressure arc discharges has been published up to now, hence no suggestions for improvement.

The right-hand side of equation (13) lacks the term $-j_R A_f/e$, describing the thermionic emission cooling, and the term $j_i\,(U - A_f/e)$, which is present in equation (14). There is also a serious problem with the evaluation of the ion current density by means of the formula $j_i = j_w - j_R$. Firstly, it does not take into account the Schottky correction. Note that latter is considered to be on the order of several tenths of electronvolt in most conditions (e.g., simulations [70]), although much higher values have been reported as well; for example, the effective work function for pure tungsten electrodes, obtained in [102] by *in situ* measurements during the operation of a free-burning atmospheric-pressure argon arc at the arc current of 100 A was 2.9 eV, which corresponds to the Schottky correction of 1.6 eV. Secondly, the evaluation of a small number (j_i) as the difference of two close numbers (j_w and j_R) is associated with a very strong increase in error.

In summary, the way of evaluation of energy flux from the plasma to thermionic cathodes in the framework of the conventional LTE model is hardly a reasonable approximation. On the other hand, the self-consistent description of interaction of high-pressure arc plasmas with thermionic cathodes is well developed by now, hence possibilities for improvement do exist. Moreover, the account of the relevant physics will simplify the workflow (except in cases where the plasma-cathode interaction is dominated by arc-related phenomena, such as plasma jets hitting the cathode surface): the cathodic part of the discharge can be computed first and this calculation will give boundary conditions for the LTE simulation of the arc bulk [18]; see discussion in section 3.5. From the technical point of view, this approach is straightforward provided that a suitable method for evaluation of integral characteristics of the non-equilibrium layer at thermionic cathodes is available; for example, the Internet tool [94], which is based on the model [70, 78, 79], can be used. Only the first step is needed in cases where the subject of study is the cathode behavior; the recent example is the work [86], where this approach was used for simulation of the change in shape of thermionic cathodes occurring during arc operation.

There seems to be a widespread opinion that the conventional LTE approach to the modelling of the high-pressure arc discharges is simpler than the one taking into account non-equilibrium near-electrode layers. This is certainly true as far as physical mechanisms taken into account are concerned. However, the conventional LTE approach is not so simple, speaking objectively, in terms of numerical realization. For example, there seems to be no commercial software which would include examples for DC arc discharges, although there are examples for LTE modelling of (electrodeless) inductively coupled discharges. One of the difficulties is the above-mentioned limitation on the minimal size of mesh elements near the electrode surfaces, which is well familiar to experienced arc modelers but is not standard from the point of view of numerical methods. On the other hand, the above-described approach [18] is numerically straightforward and may be readily realized with the use of commercial software.

5 Conclusions

The basic physics of current transfer to the electrodes of high-pressure arc discharges has been understood quite some years ago. No new physical mechanisms have been described in recent publications; the goal was rather to develop practically feasible numerical methods that adequately describe known mechanisms.

The unified approach to modelling of high-pressure arcs, which is based on solving the single set of equations, including the Poisson equation, in the whole interelectrode gap up to electrode surfaces, is highly computationally intense and its application has been limited up to now to 1D modelling of near-electrode non-equilibrium layers of high-current arcs, 1D modelling of microdischarges with low current densities, and 2D modelling of low-current arcs. On the other hand, it has delivered a number of interesting and useful, also from the methodological point of view, results.

In approaches with separate descriptions of the arc bulk and near-surface non-equilibrium layers, the physics accounted for in the non-equilibrium layers and the way in which these layers are introduced in the mathematical model of the arc on the whole need to be consistent with the physics accounted for in the arc bulk. Thus, the choice of the description of the arc bulk plasma dictates the choice of the model of the non-equilibrium layer; there is still some freedom (e.g., deviations from ionization equilibrium and charge separation in the non-equilibrium layer may be assumed to occur in the same space region or be separated in space; ion motion in the near-cathode sheath may be assumed to be collision-free or collision-dominated), but not much.

This limits the number of possible self-consistent approaches to modelling of high-pressure arc discharges and their interaction with solid surfaces: essentially, only four such approaches exist; table I. Results given by these four approaches are close to each other in many aspects; e.g., figures 4-6.

Of the four approaches, the one with the LTE description of the arc bulk coupled with the appropriate description of non-equilibrium layers on the electrodes, is by far the simplest one and has the potential of being best suited for self-consistent simulations of high-current arcs in industrial applications. In the framework of this approach, the computation domain for the LTE arc bulk equations is the whole of the interelectrode gap; the near-electrode non-equilibrium layers appear in the model as infinitesimally thin interfaces separating the computation domain from the electrode surfaces; boundary conditions for the arc bulk equations at the interfaces are obtained by solving 1D equations describing the non-equilibrium layers. In particular, the boundary conditions on thermionic cathodes can be generated by means of the tool [94]. One can hope that the account of the diffusion current in Ohm's law in the LTE arc bulk can allow a self-consistent simulation of the negative voltage and electric field reversal in front of arc anodes, an effect that has been simulated previously only by means of models taking into account deviations from ionization equilibrium.

In principle, each self-consistent approach may be applied to different regimes of current transfer to arc electrodes. In the framework of the unified modelling approach, this can be done in a straightforward way. For the other three approaches, boundary conditions on the interface separating the arc bulk from the electrode are required, which correctly describe the near-electrode physics relevant for the regime under consideration. The regime of thermionic cathode operation is studied best. Useful results have been obtained for the anode regime. Self-consistent numerical modelling of operation of non-thermionic cathodes remains a major challenge.

This work is focused on the self-consistent modelling of the physics in the immediate vicinity of the electrodes; such phenomena as impact of plasma jets over electrodes, which causes enhanced erosion and is important for applications, are beyond the scope of this work. On the other hand, a self-consistent modelling of the near-electrode physics constitutes an integral part of any self-consistent simulations of each aspect of plasma-electrode interaction.

6 Acknowledgments

The work was supported by FCT—Fundação para a Ciência e a Tecnologia of Portugal under Project UID/FIS/50010/2019 and by European Regional Development Fund through the Operational Program of the Autonomous Region of Madeira 2014–2020 under Project PlasMa-M1420-01-0145-FEDER-000016.

References

[1] A. Gleizes, Plasma Chem. Plasma Process. **35**, 455 (2015).

[2] A. B. Murphy, Plasma Chem. Plasma Process. **35**, 471 (2015).

[3] C. Chazelas, J. P. Trelles, I. Choquet, and A. Vardelle, Plasma Chem. Plasma Process. **37**, 627 (2017).

[4] A. B. Murphy and D. Uhrlandt, Plasma Sources Sci. Technol. **27**, 063001 (2018).

[5] A. J. Shirvan and I. Choquet, Welding in the World **60**, 821 (2016).

[6] M. S. Benilov, N. A. Almeida, M. Baeva, M. D. Cunha, L. G. Benilova, and D. Uhrlandt, J. Phys. D: Appl. Phys. **49**, 215201 (2016).

[7] A. I. Saifutdinov, I. I. Fairushin, and N. F. Kashapov, JETP Lett. **104**, 180 (2016).

[8] M. Baeva, M. S. Benilov, N. A. Almeida, and D. Uhrlandt, J. Phys. D: Appl. Phys. **49**, 245205 (2016).

[9] S. I. Eliseev, A. Kudryavtsev, H. Liu, Z. Ning, D. Yu, and A. S. Chirtsov, IEEE Trans. Plasma Sci. **44**, 2536 (2016).

[10] M. Baeva, Plasma Chem. Plasma Process. **36**, 151 (2016).

[11] W. Zhou, H. Guo, W. Jiang, H.-P. Li, Z.-Y. Li, and G. Lapenta, Plasma Sources Sci. Technol. **25**, 05LT01 (2016).

[12] V. A. Nemchinsky and Y. Raitses, Plasma Sources Sci. Technol. **25**, 035003 (2016).

[13] I. L. Semenov, I. V. Krivtsun, and U. Reisgen, J. Phys. D: Appl. Phys. **49**, 105204 (2016).

[14] T. Chen, C. Wang, M.-R. Liao, and W.-D. Xia, J. Phys. D: Appl. Phys. **49**, 085202 (2016).

[15] A. J. Shirvan, I. Choquet, and H. Nilsson, J. Phys. D: Appl. Phys. **49**, 485201 (2016).

[16] T. Chen, H. Li, B. Bai, M. Liao, and W. Xia, Plasma Sci. Technol **18**, 6 (2016).

[17] T. Chen, C. Wang, X.-N. Zhang, H. Zhang, and W.-D. Xia, Plasma Sources Sci. Technol. **26**, 025002 (2017).

[18] M. Lisnyak, M. D. Cunha, J.-M. Bauchire, and M. S. Benilov, J. Phys. D: Appl. Phys. **50**, 315203 (2017).

[19] N. A. Almeida, M. D. Cunha, and M. S. Benilov, J. Phys. D: Appl. Phys. **50**, 385203 (2017).

[20] M. Baeva, Plasma Chem. Plasma Process. **37**, 341 (2017).

[21] Q. Sun, C. Wang, T. Chen, and W.-D. Xia, J. Phys. D: Appl. Phys. **50**, 425202 (2017).

[22] S. Kolev, S. Sun, G. Trenchev, W. Wang, H. Wang, and A. Bogaerts, Plasma Processes Polym. **14**, 1600110 (2017).

[23] L. Pekker, Plasma Chem. Plasma Process. **37**, 825 (2017).

[24] J. Mentel, J. Phys. D: Appl. Phys. **51**, 033002 (2018).

[25] A. Khrabry, I. D. Kaganovich, V. Nemchinsky, and A. Khodak, Phys. Plasmas **25**, 013521 (2018).

[26] A. Khrabry, I. D. Kaganovich, V. Nemchinsky, and A. Khodak, Phys. Plasmas **25**, 013522 (2018).

[27] A. J. Shirvan, I. Choquet, H. Nilsson, and H. Jasak, Comput. Phys. Commun. **222**, 31 (2018).

[28] P. Liang and R. Groll, *IEEE Transactions on Plasma Science*, IEEE Trans. Plasma Sci. **46**, 363 (2018).

[29] M. A. Sargsyan, M. Kh. Gadzhiev, D. V. Tereshonok, and A. S. Tyuftyaev, Phys. Plasmas **25**, 073511 (2018).

[30] M. Baeva, AIP Advances **8**, 085322 (2018).

[31] M. Lohse, M. Trautmann, E. Siewert, M. Hertel, and U. Füssel, Welding in the World **62**, 629 (2018).

[32] A. R. Mansour and K. Hara, J. Phys. D: Appl. Phys. **52**, 105204 (2019).

[33] P. Liang, J. Phys. D: Appl. Phys. **52**, 035203 (2019).

[34] M. Baeva, D. Loffhagen, M. M. Becker, and D. Uhrlandt, Plasma Chem. Plasma Process. **39**, 949 (2019).

[35] M. Baeva, D. Loffhagen, and D. Uhrlandt, Plasma Chem. Plasma Process. (2019), 10.1007/s11090-019-10020-x.

[36] I. Choquet, Welding in the World **62**, 177 (2018).

[37] A. J. Shirvan, *Modelling of cathode-plasma interaction in short high-intensity electric arc. Application to Gas Tungsten Arc Welding*, Ph.D. thesis, Chalmers University of Technology, Gothenburg, Sweden (2016).

[38] M. Courrege, *Characterization of plasma/walls interactions in an high voltage circuit breaker*, Ph.D. thesis, Universite Toulouse 3 Paul Sabatier (2017).

[39] G. Deplaude, *Behaviour of a high-current transient electric arc: case of miniature circuit breaker*, Ph.D. thesis, Universite Paris-Saclay, France (2017).

[40] M. Lisnyak, *Theoretical, numerical and experimental study of dc and ac electric arcs*, Ph.D. thesis, GREMI, Universite d'Orleans, France (2018).

[41] M. S. Benilov, J. Phys. D: Appl. Phys. **32**, 257 (1999).

[42] M. S. Benilov, J. Phys. D: Appl. Phys. **41**, 144001 (30pp) (2008).

[43] R. M. S. Almeida, M. S. Benilov, and G. V. Naidis, J. Phys. D: Appl. Phys. **33**, 960 (2000).

[44] A. Gleizes, J. J. Gonzalez, and P. Freton, J. Phys. D: Appl. Phys. **38**, R153 (2005).

[45] V. Rat, A. B. Murphy, J. Aubreton, M. F. Elchinger, and P. Fauchais, J. Phys. D: Appl. Phys. **41**, 183001 (28pp) (2008).

[46] P. Freton, J. J. Gonzalez, Z. Ranarijaona, and J. Mougenot, J. Phys. D: Appl. Phys. **45**, 465206 (2012).

[47] J. P. Trelles, Plasma Sources Sci. Technol. **22**, 025017 (2013).

[48] J. P. Trelles, Plasma Sources Sci. Technol. **23**, 054002 (2014).

[49] D. F. N. Santos, M. Lisnyak, and M. S. Benilov, J. Phys. D: Appl. Phys. **52**, 454003 (2019).

[50] E. Fischer, Philips J. Res **42**, 58 (1987).

[51] L. Sansonnens, J. Haidar, and J. J. Lowke, J. Phys. D: Appl. Phys. **33**, 148 (2000).

[52] P. Flesch and M. Neiger, J. Phys. D: Appl. Phys. **38**, 3098 (2005).

[53] Y. Tanaka, T. Michishita, and Y. Uesugi, Plasma Sources Sci. Technol. **14**, 134 (2005).

[54] J. J. Lowke and M. Tanaka, J. Phys. D: Appl. Phys. **39**, 3634 (2006).

[55] M. Lohse, E. Siewert, M. Hertel, U. Füssel, and S. Rose, Welding in the World **59**, 705 (2015).

[56] T. Amakawa, J. Jenista, J. V. R. Heberlein, and E. Pfender, J. Phys. D: Appl. Phys. **31**, 2826 (1998).

[57] J. Haidar, J. Phys. D: Appl. Phys. **32**, 263 (1999).

[58] M. S. Benilov, IEEE Trans. Plasma Sci. **27**, 1458 (1999).

[59] J. J. Gonzalez, R. Girard, and A. Gleizes, J. Phys. D: Appl. Phys. **33**, 2759 (2000).

[60] J. Park, J. Heberlein, E. Pfender, G. Candler, and C. H. Chang, Plasma Chem. Plasma Process. **28**, 213 (2008).

[61] S. Tashiro and M. Tanaka, *22nd Symposium on Plasma Science for Materials (SPSM-22)*, Thin Solid Films **518**, 3453 (2010).

[62] M. Baeva and D. Uhrlandt, Plasma Sources Sci. Technol. **20**, 035008 (2011).

[63] H.-X. Wang, W.-P. Sun, S.-R. Sun, A. B. Murphy, and J. Yiguang, Plasma Chem. Plasma Process. **34**, 559 (2014).

[64] V. Polishchuk, High Temp. **43**, 8 (2005).

[65] M. S. Benilov and L. G. Benilova, IEEE Trans. Plasma Sci. **43**, 2247 (2015).

[66] R. K. Amirov, A. V. Gavrikov, G. D. Liziakin, V. P. Polistchook, I. S. Samoylov, V. P. Smirnov, R. A. Usmanov, N. A. Vorona, and I. M. Yartsev, IEEE Trans. Plasma Sci. **45**, 140 (2017).

[67] N. A. Almeida, M. S. Benilov, and G. V. Naidis, J. Phys. D: Appl. Phys. **41**, 245201 (26pp) (2008).

[68] N. A. Almeida, M. S. Benilov, U. Hechtfischer, and G. V. Naidis, J. Phys. D: Appl. Phys. **42**, 045210 (11pp) (2009).

[69] S. Kolev and A. Bogaerts, Plasma Sources Sci. Technol. **24**, 015025 (2015).

[70] M. S. Benilov and A. Marotta, J. Phys. D: Appl. Phys. **28**, 1869 (1995).

[71] M. S. Benilov, L. G. Benilova, H.-P. Li, and G.-Q. Wu, J. Phys. D: Appl. Phys. **45**, 355201 (2012).

[72] L. Pekker and N. Hussary, J. Phys. D: Appl. Phys. **47**, 445202 (2014).

[73] L. Pekker and N. Hussary, Phys. Plasmas **22**, 083510 (2015).

[74] M. Baeva, R. Kozakov, S. Gorchakov, and D. Uhrlandt, Plasma Sources Sci. Technol. **21**, 055027 (2012).

[75] N. K. Mitrofanov and S. M. Shkol'nik, Tech. Phys. **52**, 711 (2007).

[76] W. L. Bade and J. M. Yos, *Theoretical and Experimental Investigation of Arc Plasma-Generation Technology. Part II, Vol. 1: A Theoretical and Experimental Study of Thermionic Arc Cathodes. Technical Report No. ASD-TDR-62-729* (Avco Corporation, Wilmington, Mass., USA, 1963).

[77] M. S. Benilov and M. D. Cunha, J. Phys. D: Appl. Phys. **36**, 603 (2003).

[78] M. S. Benilov and M. D. Cunha, J. Phys. D: Appl. Phys. **35**, 1736 (2002).

[79] M. S. Benilov and M. D. Cunha, Phys. Rev. E **68**, 056407 (2003).

[80] M. S. Benilov, Plasma Sources Sci. Technol. **23**, 054019 (2014).

[81] L. Dabringhausen, O. Langenscheidt, S. Lichtenberg, M. Redwitz, and J. Mentel, J. Phys. D: Appl. Phys. **38**, 3128 (2005).

[82] A. Bergner, M. Westermeier, C. Ruhrmann, P. Awakowicz, and J. Mentel, J. Phys. D: Appl. Phys. **44**, 505203 (2011).

[83] P. G. C. Almeida, M. S. Benilov, M. D. Cunha, and J. G. L. Gomes, Plasma Sources Sci. Technol. **22**, 012002 (2013).

[84] M. Schmidt, H. Schneidenbach, and M. Kettlitz, J. Phys. D: Appl. Phys. **46**, 435202 (2013).

[85] C. Wang, W. Li, X. Zhang, M. Liao, J. Zha, and W. Xia, IEEE Trans. Plasma Sci. **43**, 3716 (2015).

[86] M. D. Cunha, H. T. C. Kaufmann, D. F. N. Santos, and M. S. Benilov, J. Phys. D: Appl. Phys. **52** (2019), accepted.

[87] "THERMCAT - On-line tool for simulation of current transfer to thermionic cathodes of high-pressure arc discharges, version 3," (2009), http://www.arc_cathode.uma.pt/tool.

[88] P. Teste, T. Leblanc, J. Rossignol, and R. Andlauer, Plasma Sources Sci. Technol. **17**, 035001 (2008).

[89] V. A. Nemchinsky and Y. Raitses, J. Phys. D: Appl. Phys. **48**, 245202 (2015).

[90] M. Redwitz, L. Dabringhausen, S. Lichtenberg, O. Langenscheidt, J. Heberlein, and J. Mentel, J. Phys. D: Appl. Phys. **39**, 2160 (2006).

[91] J. Mentel and J. Heberlein, J. Phys. D: Appl. Phys. **43**, 023002 (2010).

[92] V. L. Jorge, R. Gohrs, and A. Scotti, Welding in the World **61**, 847 (2017).

[93] M. S. Benilov, M. D. Cunha, and G. V. Naidis, Plasma Sources Sci. Technol. **14**, 517 (2005).

[94] "NCPL - On-line tool for evaluation of parameters of non-equilibrium near-cathode plasma layer in high-pressure arc plasmas," (2019), http://fisica.uma.pt/public/NCPL.

[95] H.-P. Li and M. S. Benilov, J. Phys. D: Appl. Phys. **40**, 2010 (2007).

[96] D. Santos, M. Lisnyak, M. D. Cunha, N. A. Almeida, and M. S. Benilov, in *Proc. XXII Int. Conf. on Gas Discharges and their Applications (Novi Sad, Serbia, 2nd - 7th Sept. 2018)*, Vol. 1 (2018) p. Ad. 1.

[97] M. Baeva, D. Uhrlandt, M. S. Benilov, and M. D. Cunha, Plasma Sources Sci. Technol. **22**, 065017 (2013).

[98] A. B. Murphy, J. Phys. D: Appl. Phys. **27**, 1492 (1994).

[99] C. Delalondre and O. Simonin, Coll. de Physique **51**, C5/199 (1990).

[100] P. Zhu, J. J. Lowke, and R. Morrow, J. Phys. D: Appl. Phys. **25**, 1221 (1992).

[101] A. B. Murphy, M. Tanaka, K. Yamamoto, S. Tashiro, T. Sato, and J. J. Lowke, J. Phys. D: Appl. Phys. **42**, 194006 (2009).

[102] M. Tanaka, M. Ushio, M. Ikeuchi, and Y. Kagebayashi, J. Phys. D: Appl. Phys. **38**, 29 (2005).